NUMERICAL SOLUTIONS OF MAXWELL'S EQUATIONS IN ONE AND TWO DIMENSIONS SYSTEMS BY APPLYING FINITE DIFFERENCE TIME DOMAIN (FDTD) TECHNIQUE TO STUDY ELECTROMAGNETIC WAVE PROPAGATION

Sedig S. Farhat

Department of Physics, Faculty of Science, University of Tripoli, Libya
sedigfarhat2002@yahoo.com

Abstract

The FDTD technique can be used for the transverse electric (TE) mode of a one-dimensional and transverse magmatic (TM) mode of two-dimensional in order to acquire the solutions of Maxwell's time dependent curl equations. The waves can be computed and controlled in the domain to propagate in the exact direction by simulating the presence of perfect electric conductors (PECs).

This work presents two numerical solutions in one dimension case. The first solution was acquired when high conductivity, such as the conductivity of copper material, is placed in the computational domain and compared to that of the other one when placing a PEC in the same region. The second was by applying the two different absorbing boundaries conditions.

The result obtained by the truncation condition can be compared with the first-order ABC to truncate a grid. The obtained results of the simulations were in good agreement with each other. In 2-D FDTD, the wave propagated in free space and a problem space was terminated by the first-order absorbing boundary condition (ABC) to simulate an open domain. The achieved numerical results of 2-D FDTD showed that the intensities of distributions were identical, which means that the images of the TM field's distributions appeared similar to the waves controlled between the strips.

Keywords: Maxwell's curl equations; Finite-difference time-domain (FDTD) method; transverse electric (TE) mode; transverse magnetic (TM) mode; truncation boundary condition and first-order Mur's absorbing boundary condition.

Introduction

There are many applications in electromagnetic field in which, sometimes, hard to find the exact solution. For this reason, several numerical techniques have been developed and used instead of the analytical solution. The numerical method described in this paper is the finite difference time domain (FDTD) technique, which was initially proposed by Yee S. K. in the paper published in (Yee, 1966). The method applies the finite difference concept and uses the central difference expressions to approximate the space and time derivatives to solve Maxwell's curl equations. The FDTD can solve many electromagnetic problems that are difficult to solve analytically such as in the field of antenna radiation problems and electromagnetic absorption in tissue (bio-electromagnetic) (Khitam et al., 2018 and Thomas et al., 2012). When applying the FDTD, it is very important to include the absorbing boundary conditions to improve the FDTD simulation efficiency and to obtain an accurate result. The computational domain can be terminated by either Mur's first-order absorbing boundary condition ABC or truncation condition (Biswajeet et al., 2012). They are used for the terminations of the grid in a one dimension for a comparison between the simulations while in the 2-D. The Mur's first order boundary condition is used to prevent back reflection of the wave in the space, as the reflections can affect the simulations accuracy. The ABCs must be introduced to truncate four edges around strips, as the fields will propagate in the infinite space, which surrounds the finite computational space. To simulate an infinite domain the first order, ABC needs be used to each electric field node on the boundary. This paper aims to find the approximate solutions of Maxwell's equations by studying the propagation of electromagnetic waves in one and two dimensions. The purpose of the examples in 1-DFDTD is to introduce the behaviour of electromagnetic waves when using PEC and two different boundaries, and to show how the ABCs work as well as the PEC before programming the 2-D FDTD scheme. The simulations in the 1-D FDTD by using a PEC, high conductivity and two different types of boundary conditions will be presented. The researcher expects that the same result will be obtained when applying PEC compare with a high conductivity located in the same locations in the domain. Based on the results in 1-D, numerical computational in 2-D will be conducted. The simplest way to simulate and control a wave is to use the PEC that will be demonstrated from the simulations of a one dimension system. A comparison between one dimension simulations results will be presented to show how the PEC can be used as the boundary in the 2-D, and the same methodology used in the 1-D will be used. MATLAB will be used for this purpose and to carry out the numerical calculations.

Method

MATLAB programs have been developed to study the propagation of electromagnetic waves in one and two dimensions by using the finite difference time domain (FDTD) method. This method can be applied for the transverse electric (TE) mode in a one dimension while time dependent Maxwell's curl equations can be used for solving the transverse magnetic (TM) mode in two dimensions(Jackson J., 1998):

$$\boldsymbol{\nabla} \times \mathbf{E} + \frac{\partial \mathbf{B}}{\partial \mathbf{t}} = \mathbf{0} \qquad \textbf{(1.a)}$$

$$\nabla \times \mathbf{H} - \frac{\partial \mathbf{D}}{\partial t} = \mathbf{J} \qquad \textbf{(1.b)}$$

Where D=ε E, B=μ H, J= σE. The ε, μ andσare the permittivity, permeability and conductivity of the medium, respectively.

The first part of this research describes how to solve the Maxwell's equations in a one-dimensional case whereas the second part will consider solving a problem in two-dimensional. Obtaining the electromagnetic wave in a one-dimensional system needs to be compared with the two-dimensional when inserting a PECs in both simulations. Therefore, the fields propagate in a free space in the x direction in one dimension. Two components must be computed namely the electric field oriented in y direction and the magnetic field oriented in z direction. They can be written as:

$$\frac{\partial \mathbf{E_y}}{\partial \mathbf{t}} = -\frac{1}{\varepsilon}\frac{\partial \mathbf{H_z}}{\partial \mathbf{x}} - \frac{\sigma}{\varepsilon}\mathbf{E_y} \qquad \textbf{(2.a)}$$

$$\frac{\partial \mathbf{H_z}}{\partial \mathbf{t}} = -\frac{1}{\mu}\frac{\partial \mathbf{E_y}}{\partial \mathbf{x}} \qquad \textbf{(2.b)}$$

As demonstrated in the equations (2), it can be noted that there is no variation in the y and z directions. This mode is called the transverse electric (TE) wave in a one-dimensional model to simulate the TE waves propagate for example in the x direction (Nanthini N. et al., 2015). Therefore, the computer programs were written to calculate the two field components in 1-D FDTD while using the simulation of the transverse magnetic (TM_z) mode in 2-D FDTD. There are three field components that must be calculated based on fields' locations as illustrated in Figure (1).

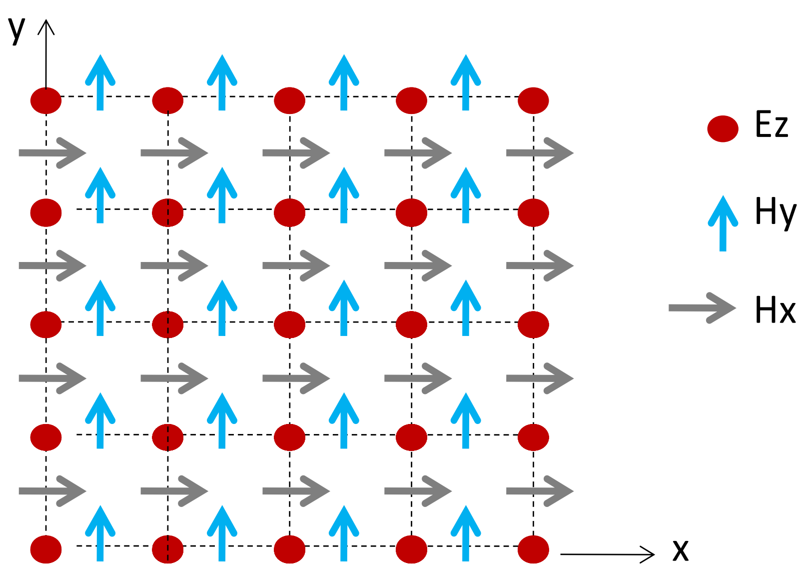

Figure (1): The Schematic Diagram of Spatial Arrangement of the Electric Field and Magnetic Field Components for Transverse Magnetic (TM_z) Wave in Two-Dimensional.

The transverse electric (TE) mode and transverse magnetic (TM_z) mode are two modes that can be used in a two-dimensional system. The latter can be called the TM_z to z-polarization; it contains the following field components: $E_z(x, y, t)$, $H_x(x, y, t)$ and $H_y(x, y, t)$. In this study, the TM_z mode was implemented and the locations of the electric and magnetic components are demonstrated in Figure (1). The set of the equations of the TM_z mode from Maxwell's equations can be expressed as the following (Yee, 1966):

$$\mathbf{E_x=E_y=0 \text{ and } H_z=0} \quad \textbf{(3.a)}$$

$$\frac{\partial E_z}{\partial t} = \frac{1}{\varepsilon_o}\left(\frac{\partial H_y}{\partial x} - \frac{\partial H_x}{\partial y}\right) \quad \textbf{(3.b)}$$

$$\frac{\partial H_x}{\partial t} = -\frac{1}{\mu_o}\frac{\partial E_z}{\partial y} \quad \textbf{(3.c)}$$

$$\frac{\partial H_y}{\partial t} = \frac{1}{\mu_o}\frac{\partial E_z}{\partial x} \quad \textbf{(3.d)}$$

The equation (3.b) provides the temporal derivative of the electric field in terms of the spatial derivative of the magnetic fields while the eq. (3.c) and eq. (3.d) provide the temporal derivative of the magnetic field in terms of the spatial derivative of the electric fields. In equations (3) it can be noticed that there is no variation in the electromagnetic fields in the z-direction and the updating equations can be obtained by applying the central difference approximation into equation (3):

$$H_x^{n+1/2}(i, j+1/2) = H_x^{n-1/2}(i, j+1/2) - \delta t/(\mu_o \delta)(E_z^n(i, j+1) - E_z^n(i, j)) \quad \textbf{(4.a)}$$

$$H_y^{n+1/2}(i+1/2, j) = H_y^{n-1/2}(i+1/2, j) + \delta t/(\mu_o \delta)(E_z^n(i+1, j) - E_z^n(i, j)) \quad \textbf{(4.b)}$$

$$E_z^{n+1}(i, j) = E_z^n(i, j) + \delta t/(\varepsilon_o \delta)((H_y^{n+\frac{1}{2}}(i+1/2, j) - H_y^{n+\frac{1}{2}}(i-1/2, j) - (H_x^{n+1/2}(i, j+1/2) - H_x^{n+1/2}(i, j-1/2)) \quad \textbf{(4.c)}$$

The superscript n is the time step whereas i and j are the space steps in the x and y directions, respectively. The equations in (4) are called discretized FDTD iteration equations; they can be used as the fields updating equations to generate the electric and magnetic fields in the computation domain in two-dimensional problem. Therefore, Maxell's equations approximated in the equations (4) will be implemented in a computer program to calculate electromagnetic waves at each time step in each pixel in the region of interest. The values of the magnetic fields will be computed depending on its pervious value and the neighbouring electric fields as an example explained for equation (4.a).The field components of the one dimension are compared with the two dimensions field components. Moreover, when using Maxwell's equations, it is often necessary to include the boundary condition to limit the region of computation domain. To simulate an infinite domain, the first order

Mur's absorbing boundary condition (ABC) will be applied at each electric field node on the boundary; it is also to minimize any reflections from four walls (Mur, 1981). The unbounded surrounding area will be simulated by applying the ABCs demonstrated on equation (5). The first-order Mur's absorbing boundary condition as the example at the boundary x=i_{max} is discretized as:

$$\mathbf{E_z^{n+1}(i_{max}, j) = E_z^{n}(i_{max-1}, j) + \frac{(c\delta t-\delta)}{(c\delta t+\delta)}(E_z^{n+1}(i_{max-1}, j) - E_z^{n}(i_{max}, j))} \qquad \textbf{(5)}$$

This equation will be used in the program to obtain and update the new field values at x=i_{max} and to update, absorbing boundary equations can be implemented at the other three edges atx=0, y=0 and y=h boundaries, respectively. These equations can be used from equation (5) in straightforward manner. The waves at the end of a computational domain will be absorbed with the first-order Mur's absorbing boundary conditions. Numerical examples are provided for one dimension and two dimensions to show the effect of the boundary condition. The boundaries can be applied to simulate the grid as open space, to obtain very good simulation results, and to limit the region of the computational domain, which can save computing time. To demonstrate the efficiency of this boundary, the researcher considered two-dimensional structure with without the ABCs as demonstrated in simulation results

Results and Discussion

The results of the numerical simulations were computed by using the FDTD technique. To simulate 1-D FDTD as the first example and D FDTD as a second example, two computer programs were developed using MATLAB programming language. The latter calculation were computed according to the distribution of the field components as shown in Figure (1) and the programs were validated by several numerical examples. With regard to one dimension case, the electric and magnetic field components were generated to compare the addition of a PEC and high conductivity in the computational domain in the same region. A point source was used to excite the domain as the sinusoidal wave operated at ten gigahertz. In a one-dimensional case, the domain was divided into 100 spatial points in a space and the signal was produced for duration of 500 time steps. The propagation behaviour of the waves was studied without including the absorbing boundary condition that compared when inserting the ABCs in the 1-D FDTD. A number of cases were reported and compared as demonstrated in Figure (2) and Figure (3). Up to this point, only one kind of boundary condition had been illustrated and the researcher could compare the results of two boundaries conditions after the domains were terminated by either the truncation boundary condition or the first-order Mur's absorbing boundary condition as shown in Figure (3) and Figure (4), respectively. Results were compared with the examples of using a PEC and high conductivity material placed in the same region in a grid. Figure (4) illustrates the wave produced in a one dimension that is similar to the one illustrated in Figure (5). The only difference is that the first simulation was placed at a high conductivity while the second simulation was placed the PEC in the first ten nodes at left side of the computational domain. One of the foremost results was that Figures (4) and (5) demonstrated the same results. This similarity indicates that electromagnetic field components were identical, the waves propagated in the positive x direction, and that there were no pulses in the regions of the high conductivity and at the PEC. The results of simulations indicated that the results obtained and the results of the simulations agree with each other. The only difference is demonstrated in Figure (2), when there is no ABC at the last electric field node on the right side of the domain, was that the reflection was obvious. The results obtained led to using Mur's first order absorbing boundary condition and a PEC in two-dimensional simulation. The effect of the boundary condition on the numerical performance when including Mur's boundary in 2-Dcan now be studied. Time data were plotted in order to compare the two examples in Figure (6) (A, B). Comparing the distributions of the TM waves when there is no an absorbing boundary is shown in Figure (6) (A). In this, the waves are propagating and reflected back into a domain and then interfering constructively and destructively with each other and generated the reflection patterns. The simulation shown in Figure (6) (B) demonstrates the effect of the first order Mur's absorbing boundary. The examples show that the difference appeared and can now be clearly observed that the performance of the Mur (ABC) provided by equation (5) is validated and the ABC made a significant impact on the results of the simulation as removed the reflection patterns as illustrated in the example provided in Figure (6) (B).

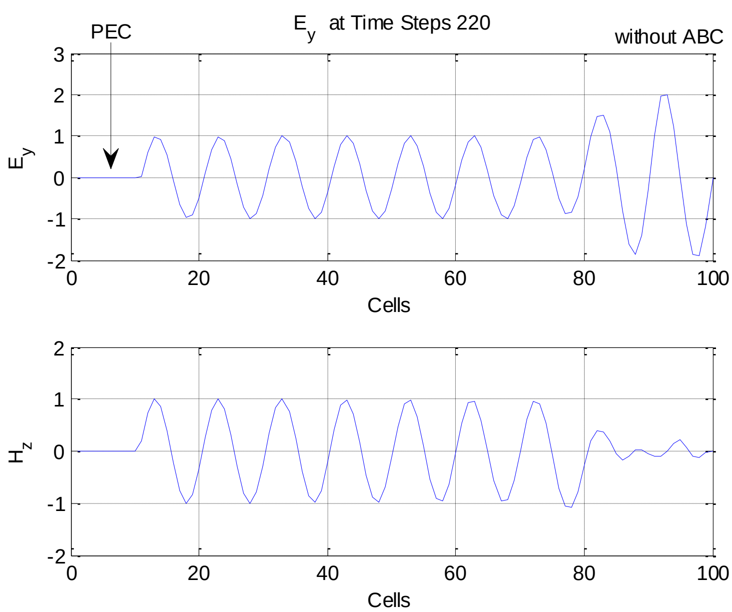

Figure (2): 1-DFDTD Simulation: the First ten Spatial Points in the Domain Filled With a PEC and There is no an Absorbing Boundary Condition at the Right Side.

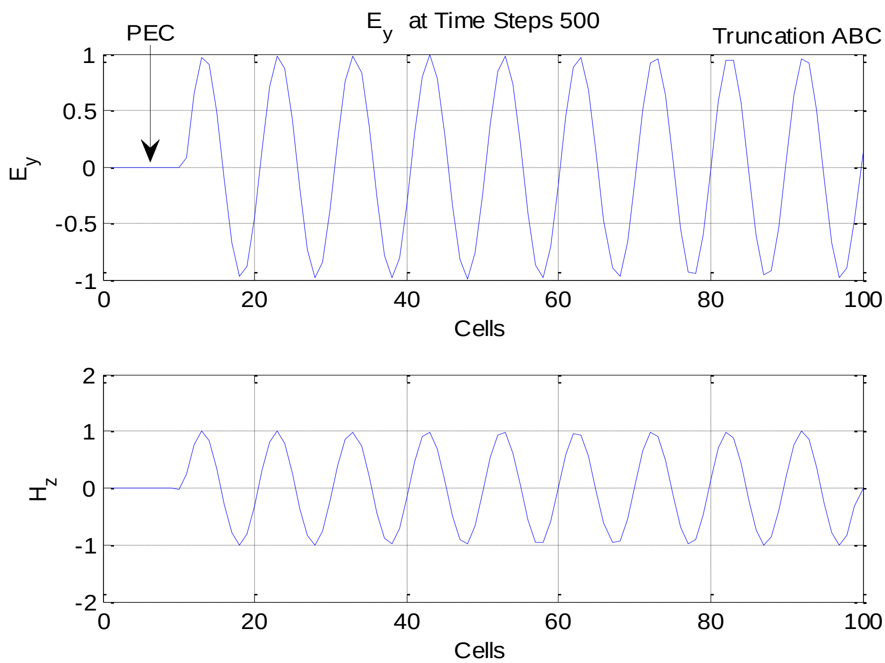

Figure (3): 1-D FDTD Simulation: the First Ten Spatial Points in the Domain Filled With PEC and the Computational Domain is Truncated in the x direction at x=h.

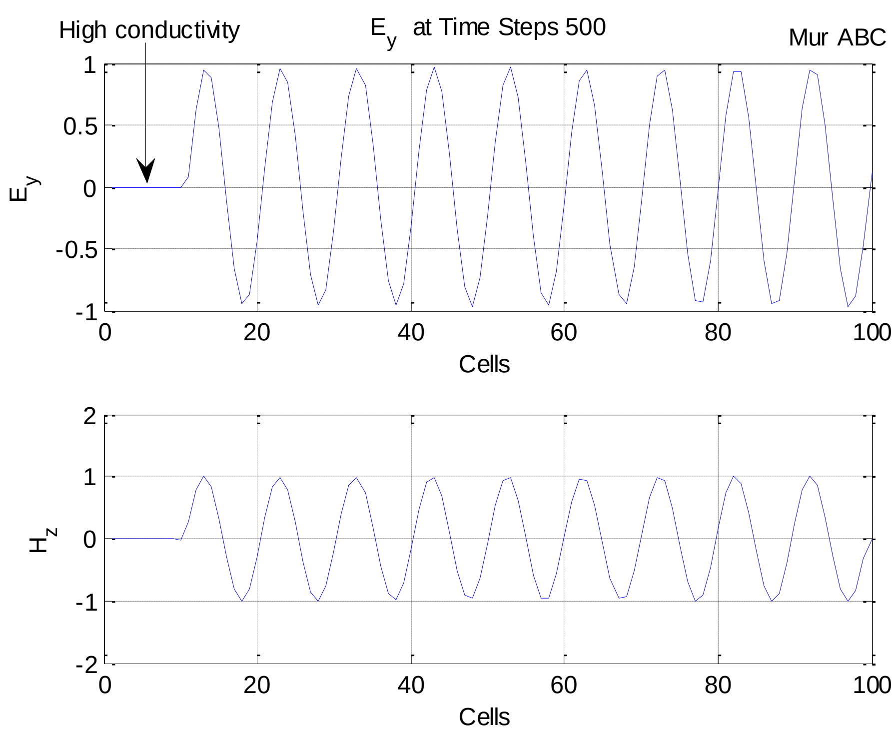

Figure (4): 1-D FDTD Simulation: the First ten Spatial Points Filled With a High Conductivity and the Right Side is Terminated by Mur's First Order ABC.

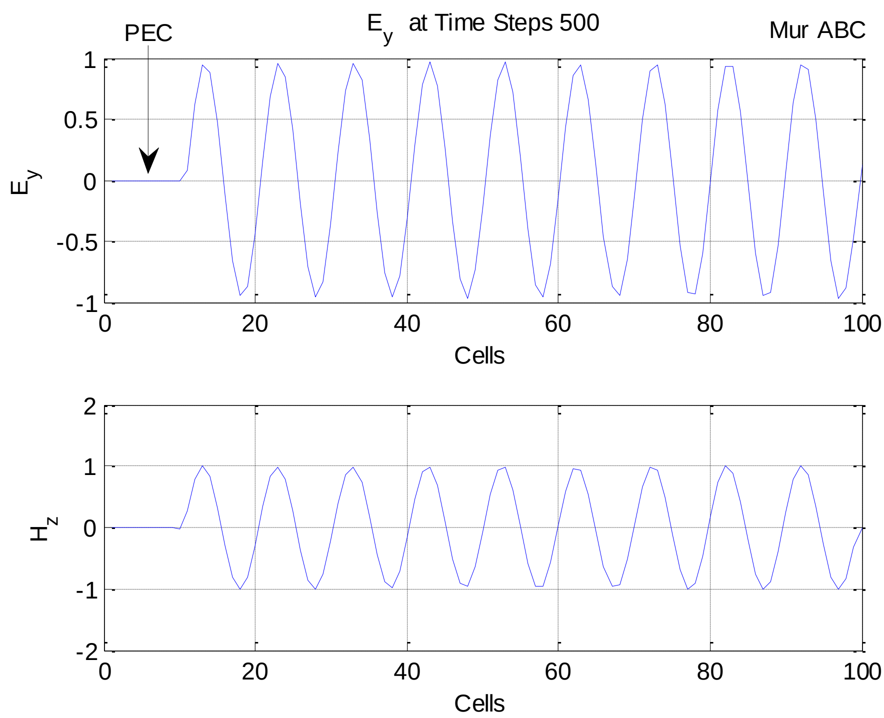

Figure (5): 1-D FDTD Simulation: the First Ten Spatial Points in the Domain Filled With PEC and the Right Side is Terminated by Mur's the First Order ABC.

It can be clearly seen that the electric field was recorded at a point in the domain as a function in time when simulating a system without the ABCs as shown in Figure (7) (A) compared with that simulation with ABCs which reached a sinusoidal steady state as shown in Figure (7) (B). As a result, the ABCs removed the reflection patterns and generated circular patterns. The result of the simulations indicates that this boundary condition provided a good performance for the two-dimensional case. It can be concluded that this is an efficient absorbing boundary condition and must be applied when simulating the 2-D FDTD problems. It was also observed that when the ABCs were not applied in 2-D simulation, the waves reflected back everywhere in the domain and they interfered with each other in the space. On the other hand, adding the first order Mur's absorbing boundary conditions at the walls caused the waves to be absorbed as well as generating very good radiation patterns as demonstrated in Figure (6) (B).

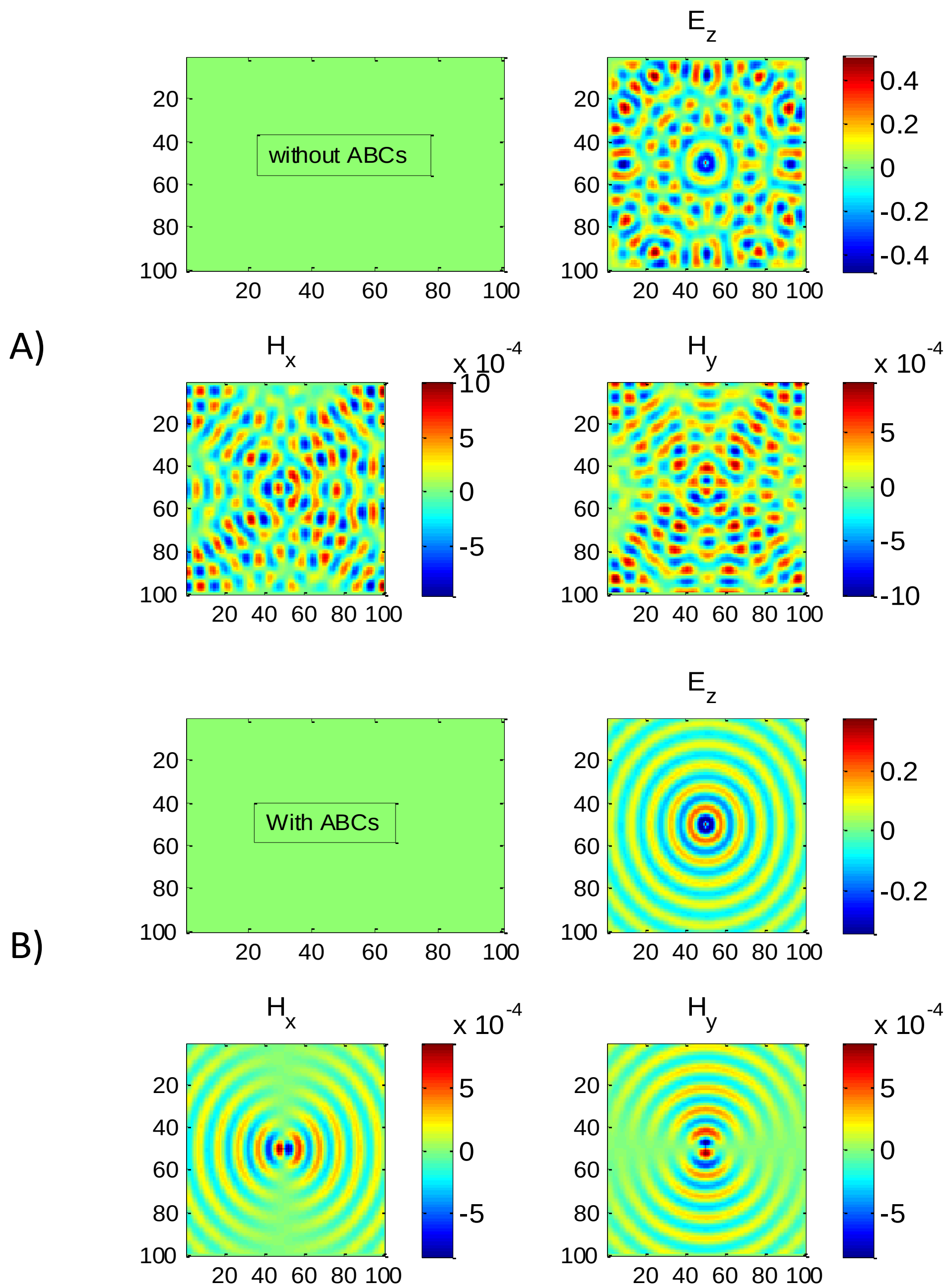

Figure (6): Comparison of the Fields Computed at n= 312 time Steps that are Propagated in two Dimensional and the E (V/m) and H (A/m) Components Calculated at all Locations at Every time. Snapshots of the TMz Distributions are Taken due to a Source with a Sinusoidal Excitation Placed in the Middle of the Domain.

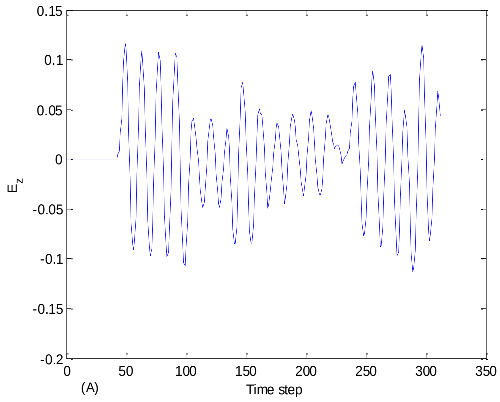

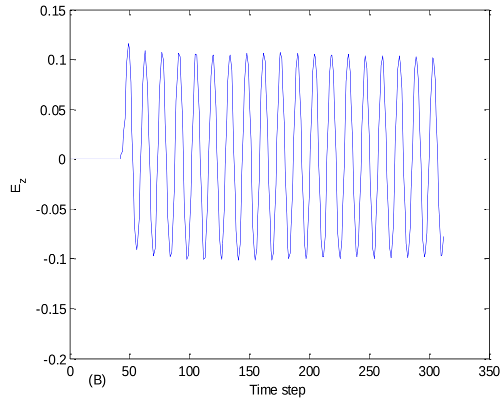

Figure (7): (A) Simulation Without the ABC Which is Unstable due to the Reflections Generated from four Edges and B) the Simulation has Reached a Steady state when applied the ABC.

Since a one dimension case absorbed the waves on the boundary as shown by the results of simulations provided in Figure (3) and Figure (4), the first-order Mur's absorbing boundary condition were applied when modelling the strips shown in Figure (8). The results of simulations in one dimension matched each other, and the examples demonstrated the fact that ahigh conductivity material can act as a PEC metal as shown in Figure (4) and Figure (5). Noticing how high conductivity can be replaced by a PEC in 1-D FDTD led the researcher to use the PECs in two-dimensional simulation to construct the structure in the region of interest by using the strips that are perfect electric conductor. Figure (8) illustrates this structure on a discrete mesh mode. Electromagnetic materials of each cell within a domain should be specified either a free space or PECs, which are assigned in each pixel. It was expected that the PEC would act as a metal layer as explained when simulated in a one-dimensional simulation. By using this setting, there was no excitation inside PECs regions.

The electric fields components must have zeros values at the boundaries in the PECs regions. The structure in the first model consisted of two parallel strips (PECs) and the length of each was considered to be 45 cells in x direction and the distance between two strips was about 9 cells in y direction, see Table (1) and the geometry of the considered structure shown in Figure (8). The simulation of a two-dimensional system is only in the x and y directions and can be solved by 100×100 point lattice. The space discretization step must be smaller than the wavelength. The spatial discretization could be provided as ten sample points per wavelength and time step was based on the Courant condition for 2-D FDTD. The condition for stability shown in (Otman et al., 2017) was adopted in this study for the two-dimensional simulation to satisfy the stability condition. There are hard source and soft source excitation (Bojan et al. 2015 and Mansour Abadi et al., 2008). A hard source can be used to excite the computational domain by using a sinusoidal wave, which is operated at a 10 GHz in the simulations. The excitation of a wave is applied to **E_z** field, i.e. polarized in the z direction. From Figure (9), it can be observed that the electromagnetic field was guided until it reached the end of the structure then it started propagation until it hit the right walls. Then, the electromagnetic waves reflected back into a domain and reflection patterns were generated because there was no ABC included on the right side. Figure (10) demonstrates how to remove the reflection patterns by added the ABC on the right side. The propagation of signals in the left or right side and uniformity of the signals have been studied in this study. In the first model, the domain, which was excited by a sinusoidal source, was placed at the left side proximity and was very close to the left side of the structure; the electromagnetic waves were leaving the structure aperture at the right end. In the second simulation, the source was placed close to the right side and the electromagnetic waves were leaving the structure aperture at the left end as shown in Figure (10) and Figure (11), respectively.

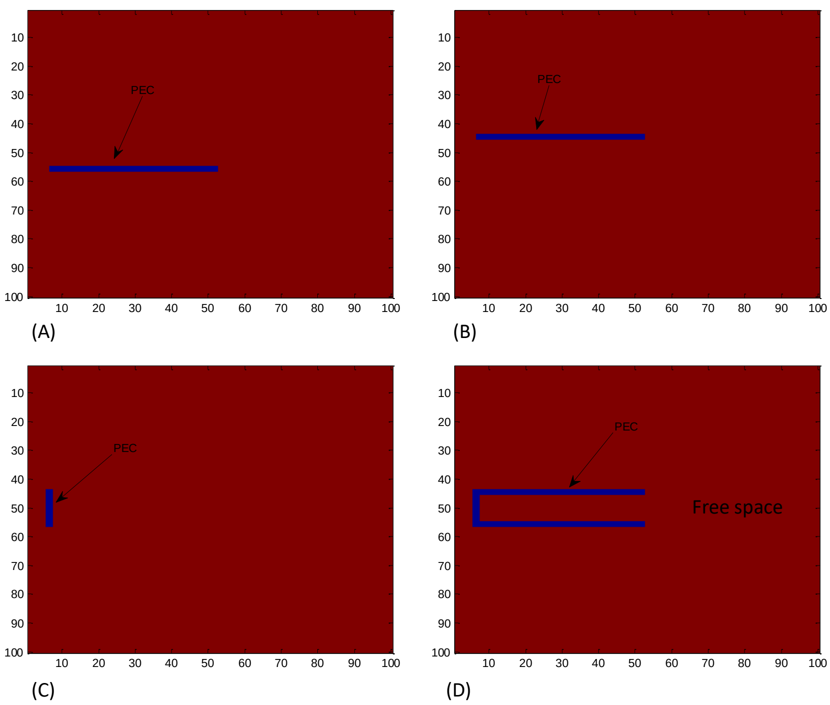

Figure (8): This kind of Configuration of the Strips and the Geometry is Constructed in the 2-DFDTD System as a Mesh Mode by Inserted the Strips Have Properties of Perfect Electric Conductors (PECs) in the Grid and Seta Free Space Everywhere Surround the Structure.

Table (1): The strips Set as the Perfect Electric Conductors (PECs) in the First Simulation.

Upper strip	E_z (7:52, 55)=0
Lower strip	E_z (7:52, 45)=0
Left strip	E_z (6:7, 45:55)=0

Within the third simulation, the source was placed in the middle of a structure as shown in Figure (12). The wave propagated inside a structure in 2-D was opened from both sides. The field components were propagated and controlled between two strips. The simulation ran in 2-D FDTD and the time domain data was recorded at a spatial point during the calculation in order to observe a steady state of the simulation see Figure (13). It was noticed that the wave was updated on 1-D system as a point by point and the signal propagated in the x direction. This can be compared with2-D simulation as shown in Figure (10) and Figure (11), where the signals were updated in the computation domain as a pixel by pixel in the structure between two strips. From Figure (10) and Figure (11), the signals propagated on the right direction and left direction, respectively. The main difference between the two simulations is that placing the source at the end of the left side and second simulation the source placed at the end of the right side. The perfect electric conductor at left and right sides will reflect the signals in the opposite direction. It can be seen that these results were obtained as the same instant in time. The perfect electric conductor acted the same as a high conductivity material, as demonstrated in the simulation results in 1-D system. Figure (5) and Figure (10) show that very good uniformity can be achieved when the signals reach a steady state and use the same distributions and other possible application when placing a source at the right and the same result is obtained as shown in Figure (11).

Moreover, the electric field component could be recorded at a point between two parallel strips during iteration as demonstrated in Figure (13), which demonstrates that the simulation reached the steady state after n time steps. It is observed from Figure (12) that the wave is controlled to propagate between two parallel strips and the waves are propagating bilaterally, in positive and negative directions. The type of this structure leads to concentrating the signals between two strips until the ends of structures as much as possible then the waves will leave the aperture. Field components can be concentrated by using the structure shown in Figure (8) and good homogeneity of TM_z distribution achieved in all simulation. It can be observed that when electromagnetic waves reach the end of the structure after n time steps, the field components begin updating in the end of the aperture in each pixel, the signals propagate at the right side, and at the end of aperture the signal spread out everywhere in the computational domain as shown in Figures, (10), (11) and (12). It can be said that by setting the strips that have properties of a perfect electric conductor; the TM wave can be controlled to propagate in free space in the x-y directions in two dimensions system.

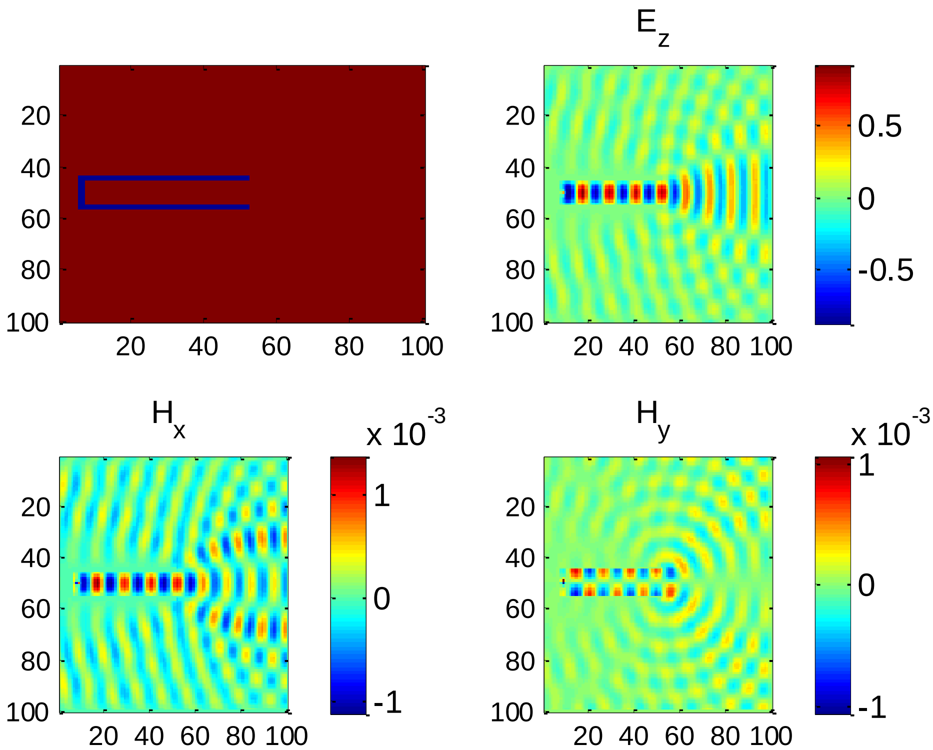

Figure (9): Snapshot is Taken at 312 Time steps and the E (V/m)and H (A/m) Waves are Propagating at the Right Side Until Reaching to the Right wall then Starting Reflected Back into a Domain as there is no ABC on the Right side of a Domain.

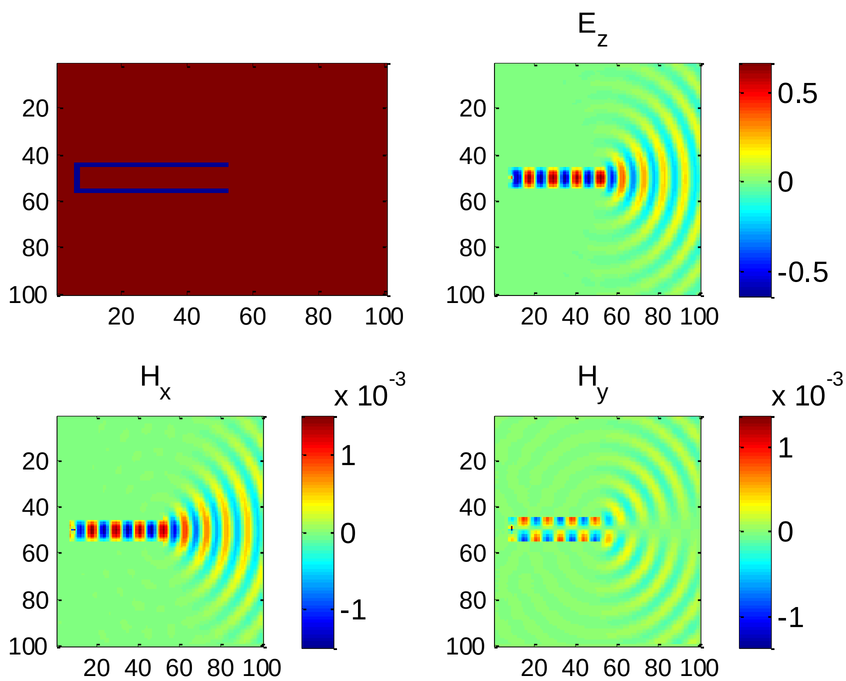

Figure(10) :Snapshot is Taken at 312 Time Steps and the TM_z wave, E (V/m) and H (A/m) are Propagating at the Right Side.

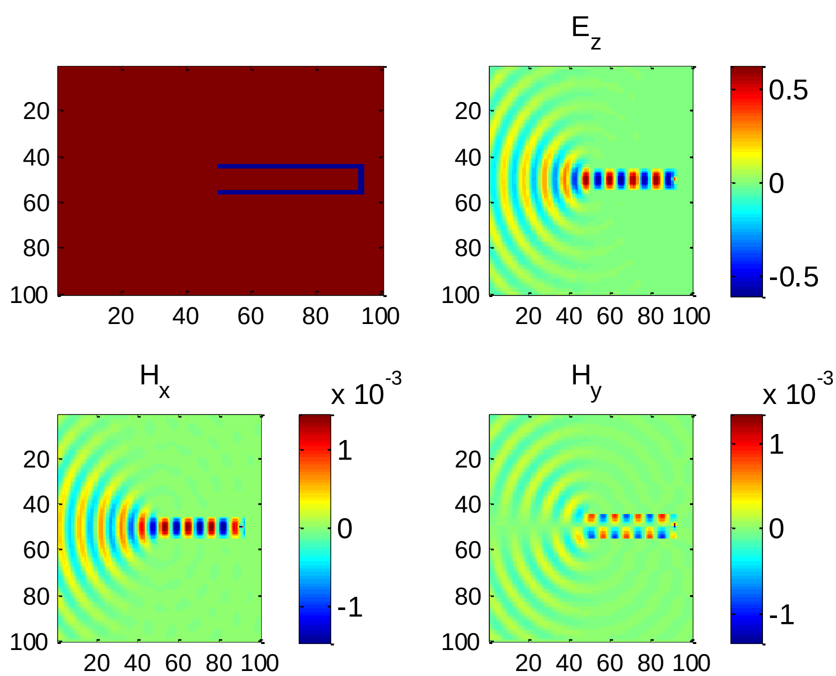

Figure(11) : Snapshot is Taken at 312 time Steps and the TM_z wave, E (V/m) and H (A/m)are Propagating at the Left side.

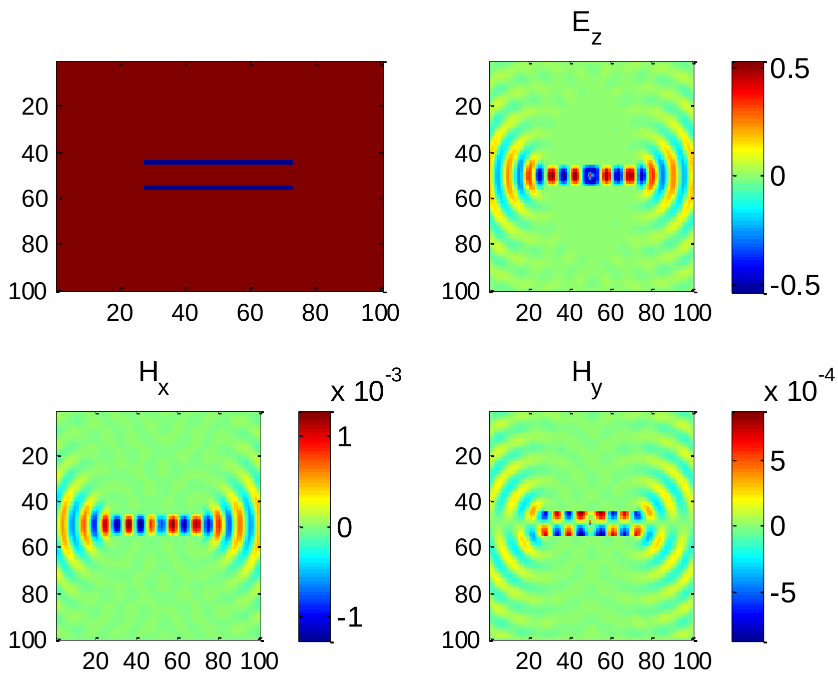

Figure (12): Snapshot is Taken at 312 Time Steps and the TM$_z$ wave, E (V/m) and H (A/m) are Propagating Bilaterally, Positive and Negative Directions.

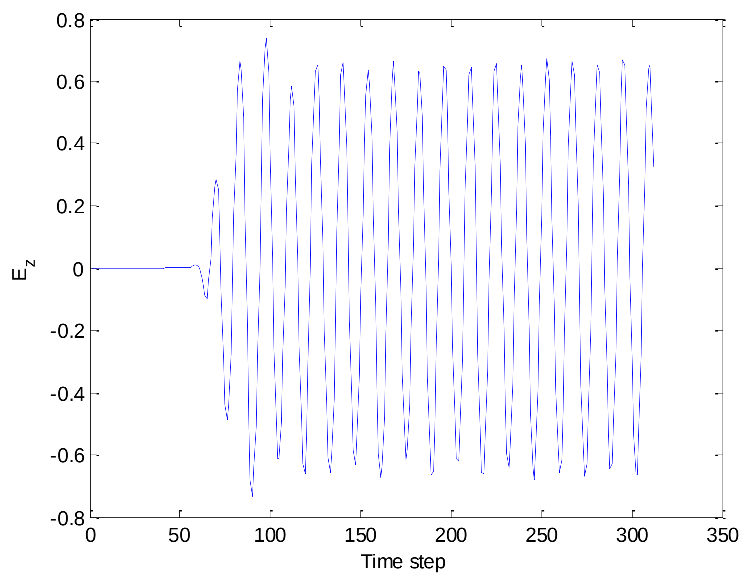

Figure (13): The Simulation Reached a Steady State due to the Source Placed in Side the Structure.

Conclusions

The FDTD method was a very powerful and efficient technique to solve Maxwell's equations in the time domain as explained when implementing of FDTD method in a one-dimensional and two-dimensional cases. The method was used for a numerical study to find the solutions of that would be difficult to solve analytically. We provided many numerical examples and discussed the absorbing boundary conditions (ABCs)that were applied to truncate the computational domain in order to simulate an open domain. All simulations were performed in this work adapted the first-order Mur's absorbing boundary condition. The results of the simulations demonstrated that successfully the ABCs implemented, the electromagnetic fields generated, the waves propagated and reached a steady state solutions in a structure in two-dimensional case and the waves were controlled by using two parallel strips. The results indicate that the method can be used to simulate complicated structure.

References

- Biswajeet M. and Dinesh V. (2012). Application of finite difference time domain to calculate the transmission coefficient of an electromagnetic wave impinging perpendicularly on a dielectric interface with modified MUR-I ABC. Defence Science Journal, **62**, 228-235.

- Bojan D., Bojana N., Slavoljub A. and Nebojsa R. (2015). Optimization of excitation in FDTD method and corresponding source modeling. Radio engineering journal, **24**, 10-16.

- Jackson J., (1998). Classical electrodynamics. United states America.

- Khitam Y. E., Sami A. A., and Mohammed M. S. (2018). 3D-FDTD Head Model Exposure to Electromagnetic Cellar Phones Radiation, American journal of electromagnetic and applications, **6**, 42-48.

- Mur, G. (1981). Absorbing Boundary Conditions for the Finite Difference Approximation of the Time Domain Electromagnetic Field Equations, IEEE Transactions on Electromagnetic Compatibility, EMC-**23**, 377-382.

- Mansour Abadi M. and Pourkazemi A. (2008). FDTD hard source and soft source reviews and modifications. Progress in electromagnetic research journal, **3**, 143-160.

- Nanthini N. and Ramanathan V. (2015). electromagnetic field propagation analysis in free space using finite difference time domain method (FDTD), international journal of innovative research in computer and communications engineering, **3**, 144-151

- Otman S. and Ouaskit S. (2017). FDTD simulations of surface Plasmon using the effective permittivity applied to the dispersive media. American journal of electromagnetic and applications, **5**, 14-19.

- Thomas V. and John G. (2012). RF coils for MRI. John Wiley and sons.

- Yee S. K. (1966). Numerical Solution of Initial Boundary Value Problems Involving Maxwell's Equations in Isotropic Media. IEEE Transactions Antennas and Propagation, **14**, 302-307.